Supplemental Information of Mechanisms of bismuth-activated near-infrared photoluminescence - a first-principles study on the $MX\mathrm{Cl}_3$ series

Qiaoling Chen,[1,2,3] Weiguo Jing,[1,2,3] Yau-Yuen Yeung,[4] Min Yin,[5,*] and Chang-Kui Duan[1,2,3,†]

[1] *Hefei National Laboratory for Physical Sciences at the Microscale and School of Physical Sciences, University of Science and Technology of China, Hefei 230026, China*
[2] *CAS Key Laboratory of Microscale Magnetic Resonance, University of Science and Technology of China, Hefei 230026, China*
[3] *Synergetic Innovation Center of Quantum Information and Quantum Physics, University of Science and Technology of China, Hefei 230026, China*
[4] *Department of Science and Environmental Studies, The Education University of Hong Kong, 10 Lo Ping Road, Tai Po, NT, Hong Kong, China*
[5] *CAS Key Laboratory of Strongly-Coupled Quantum Matter Physics, University of Science and Technology of China, Hefei 230026, China*

NOTE 1 CHARGE CORRECTIONS

Defect calculations are often performed by periodic boundary conditions within desity-functional theory (DFT) and the periodic translations introduce the electrostatic interaction of the defect and its images when the defects has net charge. For computational costs, *post hoc* corrections to final energy is employed and several approaches have been proposed to overcome this problem, such as Makov and Payne (MP), Freysoldt, Neugebauer, and Van de Walle (FNV), and Lany and Zunger (LZ). Besides, the use of periodic boundary conditions also creates an additional problem that the bulk electrostatic potential is not properly recovered far from the defect. Recently, Durrant *et al.* proposed that the combination of the Lany-Zunger correction for the charged defects due to image charge and the potential alignment between neutral systems (the original host supercell and the unrelaxed supercell containing the defect) can yield accurate corrections for cubic supercells [1]. Hence, this approach is adopted here for Bi:$MX\mathrm{Cl}_3$ systems.

For the image charge correction, the Lany-Zunger (LZ) correction is given by

$$E_{\mathrm{corr}}^{\mathrm{LZ}} = (1+f)\frac{q^2\alpha_M}{2\epsilon L} \tag{1}$$

where $1+f \approx 2/3$, Madelung-like constant $\alpha_M = 2.837$ for a cubic supercell, ϵ is the dielectric constant and $L = \Omega^{1/3}$ is the linear supercell dimension (Ω is the volume of supercell). Since the ionic relaxation provides additional dielectric screening of the interactions between the replicas, the static dielectric constant ϵ_0 is applied.

For the potentail alignment, Durrant *et al.* [1] proposed that the potential shift caused by change in atomic composition is the dominant remaining finite-size error once the image charge interaction correction has been applied. The potential difference between the neutral supercell containing the defects (unrelaxed) and the perfect supercell are calculated. Fig. S1 shows the potential difference of defects in $\mathrm{KMgCl_3}$ crystal and take defect of $\mathrm{Bi_K}$ for example, the correction for an electron is $q\Delta V = -0.04$ eV, i.e., $\Delta V = 0.04$ V. The detailed correction to total energies are listed in Table S1.

NOTE 2 DEFECT FORMATION ENERGY

The formation energy of a defect in charge state q is defined as [2]

$$E^f[X^q] = E_{\mathrm{tot}}[X^q] - E_{\mathrm{tot}}[\mathrm{bulk}] - \sum_i n_i\mu_i + qE_F \tag{2}$$

Here, we take the $\mathrm{KMgCl_3}$ crystal in the condition of Fig. 1 as an example to discuss the computational details. First, the geometric relaxation is applied for $\mathrm{KMgCl_3}$ primitive cell. A supercell is constructed based on the relaxed primitive cell, where new-base vectors are [2**a**, 2**b**, 2**c**] for $\mathrm{KMgCl_3}$. $E_{\mathrm{tot}}[\mathrm{bulk}]$ is the total energy of the perfect supercell. $\mathrm{Bi_K}$, $\mathrm{Bi_{Mg}}$, V_{K}, V_{Mg}, V_{Cl} defects are considered and Tabel S5 lists the differences in the number of atom species n_i between the supercell containing the defect and perfect supercell. The geometric relaxation with fixing supercell volume is applied to the supercell containing a defect in charge state q and the total energy is obtained as $E_{\mathrm{tot}}[X^q]$, where the charge corrections should be included. The chemical potentials can be expressed by $\mu_i = \mu_i^0 + \Delta\mu_i$ and $\Delta\mu_i$ is the excess chemical potential to their reference state and can be viewed as a tunable term to describe the experimental growth condition. The reference chemical potential μ_{Cl}^0 is obtained as -1.91 eV with GGA-PBEsol method. It is half of the energy of an isolated chlorine molecule, which is calculated by placing an chlorine molecule in a 10*10*10 Å^3 supercell. In the condition of Fig. 1, the chemical potential $\mu_{\mathrm{Cl}} = \mu_{\mathrm{Cl}}^0 + \Delta\mu_{\mathrm{Cl}}$ is -2.91 eV. Similarly, the reference chemical potentials μ_{KCl}^0 and $\mu_{\mathrm{MgCl_2}}^0$ are -7.03 eV and -11.35 eV from the total energy calculations for KCl and $\mathrm{MgCl_2}$ crystals, respectively. Then the chemical potentials $\mu_{\mathrm{KCl}} = \mu_{\mathrm{KCl}}^0 + \Delta\mu_{\mathrm{KCl}}$ and

* yinmin@ustc.edu.cn (M. Yin)
† ckduan@ustc.edu.cn (C.-K. Duan)

$\mu_{MgCl_2} = \mu^0_{MgCl_2} + \Delta\mu_{MgCl_2}$ are -7.08 eV and -11.35 eV, when $\Delta\mu_{MgCl_2} = 0$ and $\Delta\mu_{KCl} = \Delta H_{KMgCl_3}$ correspondingly in the case of acidic chlorine $MgCl_2$ being residule. Thus, μ_K and μ_{Mg} can be calculated by $\mu_K = \mu_{KCl} - \mu_{Cl}$ = -4.17 eV and $\mu_{Mg} = \mu_{MgCl_2} - 2\mu_{Cl}$ = -5.53 eV. The defect formation energy is obtained as a linear function of the Fermi energy (E_F) that is referenced to the valence-band maximum (VBM), as shown in Fig. 1. The same procedures are conducted for the defects in other $MXCl_3$ hosts. All data are availible on request from the corrsponding author.

NOTE 3 THE LUMINESCENCE OF Bi^{3+}

Previous study has reported the luminescence properties of Bi^{3+} in $CsMgCl_3$ and $CsCdBr_3$ crystals in experiments to show violet to blue light [3]. As plotted in Fig. S5, the unoccupied 6s character level and lowest 6p KS orbital character level are calculated with PBE0 method, which is obtained by removing a 6s electron in the equilibrium structure of Bi^{3+} ground state. The energy difference corresponds to the theoretical zero-phonon-line of the transitions, which is roughly the average of excitation and emission energies. These are consistent with experiments. Besides, $CsCdCl_3$:Bi^{3+} is applied to interpret the luminescence of Bi^{3+} in $CsCdBr_3$ crystal because Bi^{3+} coordinated with similar Cd ligands. Since the valence band maximum is dominated by the halogen elements, Br has higher 3p than Cl with 2p orbital energy. And thus, Bi^{3+} in $CsCdBr_3$ crystal shows more preferable of the charge transfer transition and Bi^{3+} in $CsMgCl_3$ crystal has both the intra-ionic electron transitions and the charge transfer transition. While more detailed calculation is needed for clarify, we can nevertheless exclude that Bi^{3+} exhibits the NIR emission under red light excitation.

[1] T. R. Durrant, S. T. Murphy, M. B. Watkins, and A. L. Shluger. Relation between image charge and potential alignment corrections for charged defects in periodic boundary conditions. *The Journal of chemical physics*, 149(2):024103, 2018.

[2] Christoph Freysoldt, Blazej Grabowski, Tilmann Hickel, Jörg Neugebauer, Georg Kresse, Anderson Janotti, and Chris G. Van de Walle. First-principles calculations for point defects in solids. *Reviews of modern physics*, 86(1):253, 2014.

[3] A. Wolfert and G. Blasse. Luminescence of s^2 ions in $CsCdBr_3$ and $CsMgCl_3$. *Journal of Solid State Chemistry*, 55(3):344–352, 1984.

TABLE S1. The charge corrections to total energies in $MX\mathrm{Cl}_3$ crystals

		$KMgCl_3$	$KCdCl_3$	$RbMgCl_3$	$RbCdCl_3$	$CsMgCl_3$	$CsCdCl_3$
ϵ_0		7.05	8.27	9.59	7.69	9.14	11.53
$E^{\mathrm{LZ}}_{\mathrm{corr}}$		$0.12q^2$	$0.10q^2$	$0.10q^2$	$0.11q^2$	$0.10q^2$	$0.08q^2$
ΔV	Bi_M	0.04	0.04	0.05	0.03	0.03	0.02
	Bi_X	0.19	0.18	0.18	0.16	0.18	0.33
	V_M	-0.11	-0.11	-0.14	-0.11	-0.16	-0.18
	V_X	-0.09	-0.12	-0.11	-0.10	-0.07	-0.11
	V_{Cl}	-0.03	0.00	-0.04	-0.01	-0.05	0.02

TABLE S2. Calculated and experimental geometrics of $MX\mathrm{Cl}_3$ hosts (units: Å)

		Calculated				Measured			
Host	space group	a	b	c	volume (Å^3)	a	b	c	volume (Å^3)
$KMgCl_3$	Pbnm	6.883	6.976	9.848	472.87	6.954	6.971	9.922	480.98
$KCdCl_3$	Pnma	8.743	3.977	14.549	505.90	8.792	3.994	14.599	512.65
$RbMgCl_3$	$P6_3/mmc$	7.047	7.047	17.491	752.34	7.095	7.095	17.578	766.31
$RbCdCl_3$	Pnma	8.923	4.020	14.963	536.70	8.962	4.034	14.980	541.57
$CsMgCl_3$	$P6_3/mmc$	7.208	7.208	6.139	276.23	7.260	7.260	6.180	282.09
$CsCdCl_3$	$P6_3/mmc$	7.371	7.371	18.437	867.47	7.403	7.403	18.406	873.59

TABLE S3. Wyckoff position and the corresponding average bond length with Cl in $MX\mathrm{Cl}_3$ hosts

	$KMgCl_3$	$RbMgCl_3$	$CsMgCl_3$	$KCdCl_3$	$RbCdCl_3$	$CsCdCl_3$
M sites	C_s	D_{3h}/C_{3v}	D_{3h}	C_s	C_s	D_{3h}/C_{3v}
M-Cl (Å)	3.50	3.55/3.55	3.69	3.30	3.40	3.72/3.72
X sites	C_i	D_{3d}/C_{3v}	D_{3d}	C_s	C_s	D_{3d}/C_{3v}
X-Cl (Å)	2.50	2.48/2.48	2.49	2.64	2.64	2.60/2.61

TABLE S4. Formation enthalpy and chemical potentials used in Fig. 1 (units: eV)

	$KMgCl_3$	$RbMgCl_3$	$CsMgCl_3$	$KCdCl_3$	$RbCdCl_3$	$CsCdCl_3$
$\Delta H_{MX\mathrm{Cl}_3}$	-0.052	-0.162	-0.365	-0.141	-0.199	-0.275
$\Delta\mu_{M\mathrm{Cl}}$	-0.052	-0.162	-0.365	-0.141	-0.199	-0.275
$\Delta\mu_{X\mathrm{Cl}_2}$	0	0	0	0	0	0
$\Delta\mu_{\mathrm{Bi}}$	-0.794	-0.794	-0.794	-0.794	-0.794	-0.794

TABLE S5. The differences in the number of atom species n_i of different defects in $MX\mathrm{Cl}_3$ (M =K, Rb, Cd; X =Mg, Cd) hosts

	Bi_M	Bi_X	V_M	V_X	V_{Cl}
n_M	-1	0	-1	0	0
n_X	0	-1	0	-1	0
n_{Cl}	0	0	0	0	-1
n_{Bi}	1	1	0	0	0

TABLE S6. Excitation and emission energies obtained by different calculation methods and experiments (units: eV)

	Exc.-Expt.	Exc.-CDFT	Exc.-AIMP	Emi.-Expt.	Emi.-CDFT	Emi.-AIMP[a]
$\mathrm{KMgCl_3}$	2.05/1.95	1.87/1.56	2.18/2.33	1.30	1.54	1.51
$\mathrm{RbMgCl_3}$-Rb1	2.03/1.92	1.80/1.69	2.26/2.28	1.37	1.63	1.57
$\mathrm{RbMgCl_3}$-Rb2	2.03/1.92	1.80/1.69	2.23/2.27	1.37	1.62	1.59
$\mathrm{CsMgCl_3}$	2.05/1.90	1.91/1.63	2.24/2.31	1.35	1.48	1.40
$\mathrm{KCdCl_3}$	2.02/1.81	1.69/1.46	2.15/2.29	1.31	1.25	1.34
$\mathrm{RbCdCl_3}$	2.05/1.85	1.90/1.56	2.12/2.34	1.22	1.25	1.20
$\mathrm{CsCdCl_3}$-Cs1	2.02/1.90	1.83/1.68	2.22/2.29	1.27	1.41	1.32
$\mathrm{CsCdCl_3}$-Cs2	2.02/1.90	2.30/1.67	2.15/2.63	1.27	1.40	1.11

[a] Calculated by the first excited energy in the ground state and then substract the Stokes shift, which is roughly estimated by the results of CDFT method.

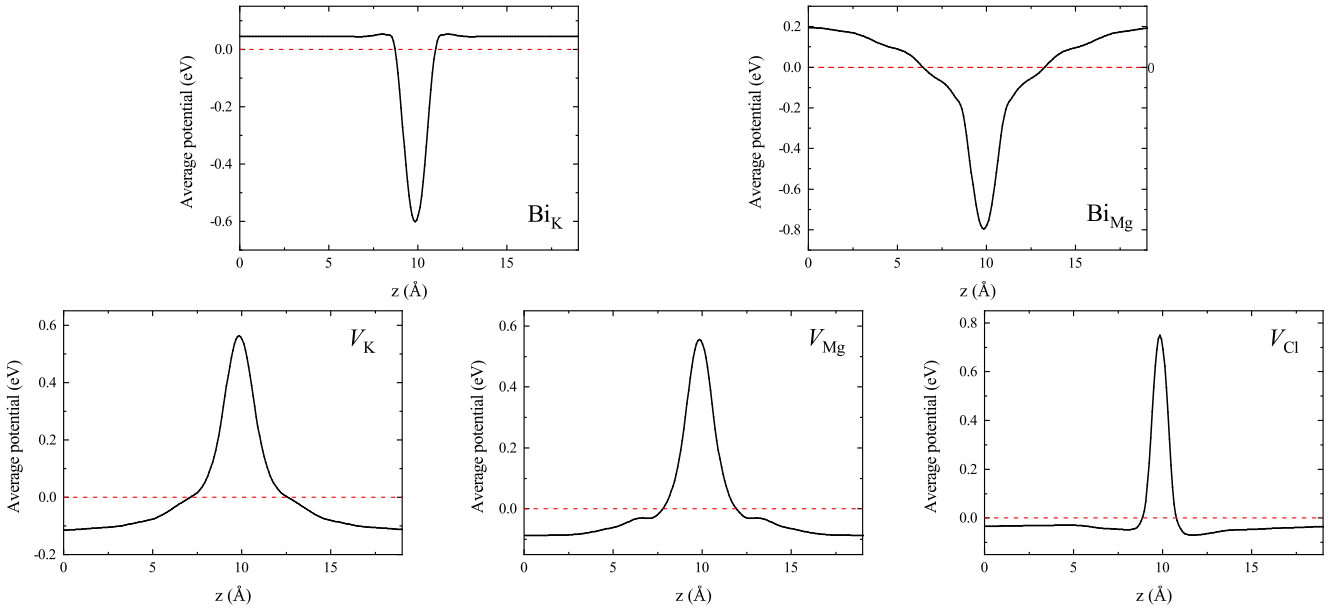

FIG. S1. The potential difference between the neutral supercell containing the defects of $\mathrm{Bi_K}$, $\mathrm{Bi_{Mg}}$, V_{K}, V_{Mg}, V_{Cl} (unrelaxed) and the perfect supercell in $\mathrm{KMgCl_3}$ crystal.

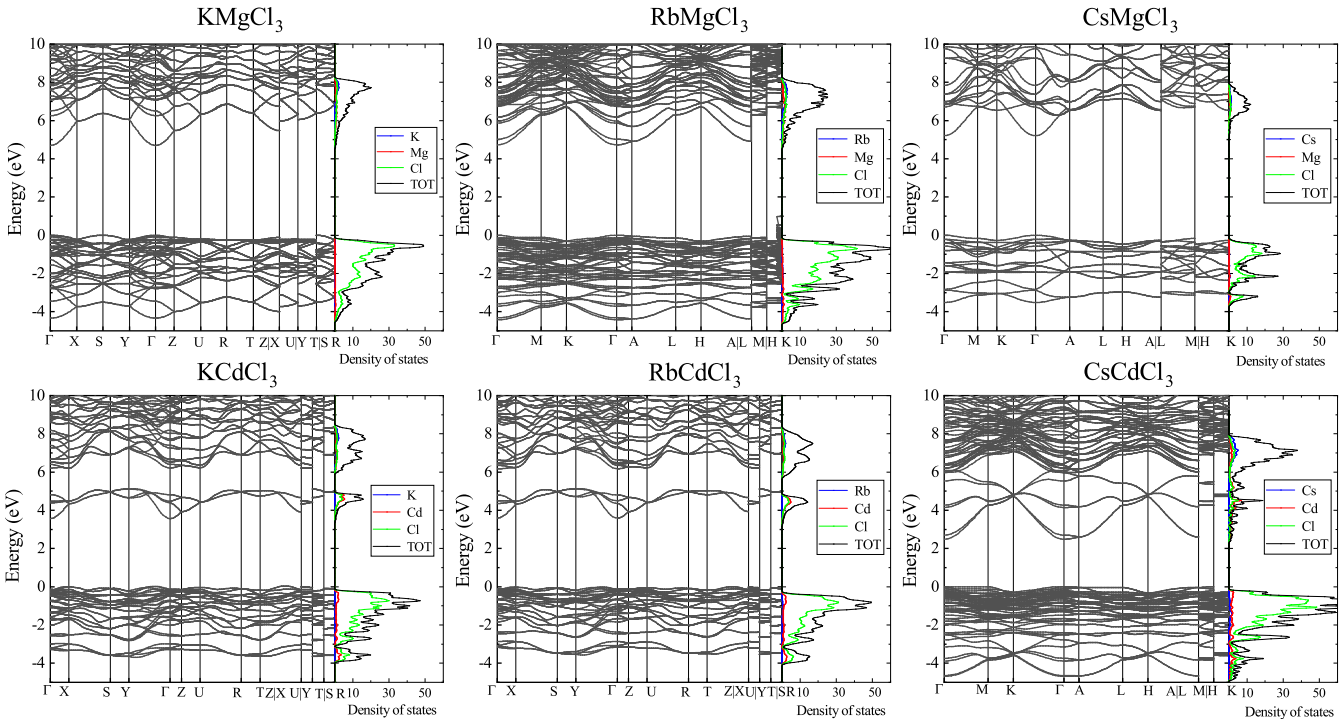

FIG. S2. Band structure and density of states of $MX\mathrm{Cl}_3$ crystals

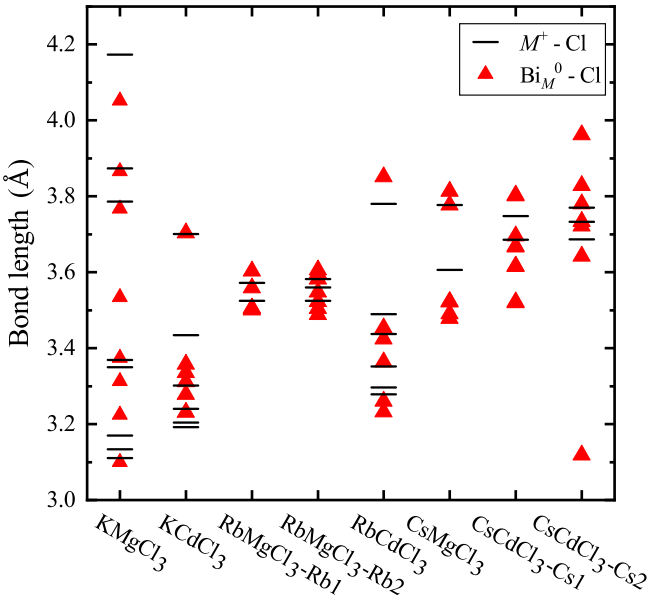

FIG. S3. The bond lengths of M^+ - Cl (black line) and Bi_M^0 - Cl (red triangle) in $MX\mathrm{Cl}_3$ (M = K, Rb, Cs; X = Mg, Cd) crystals.

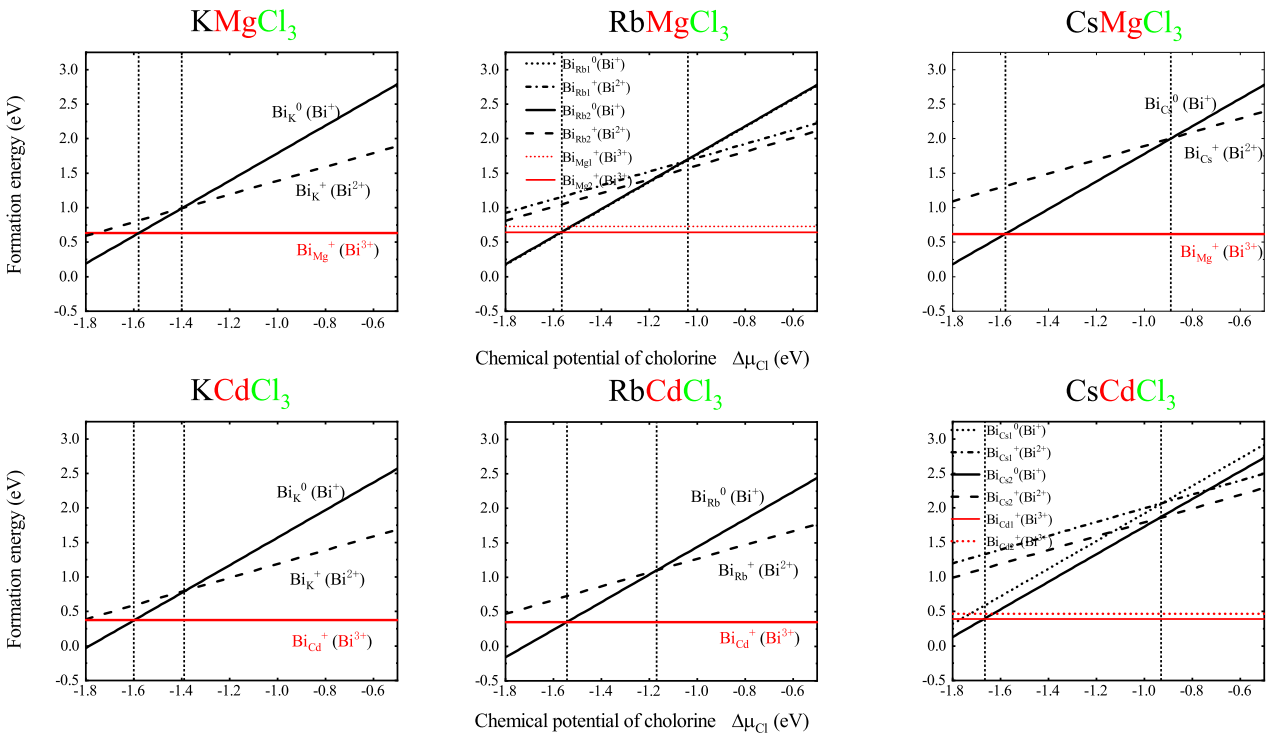

FIG. S4. Calculated formation energies of Bismuth defects as a function of chemical potential of cholorine $\Delta\mu_{\mathrm{Cl}}$ in $MX\mathrm{Cl}_3$ (M = K, Rb, Cs; X = Mg, Cd) crystals.

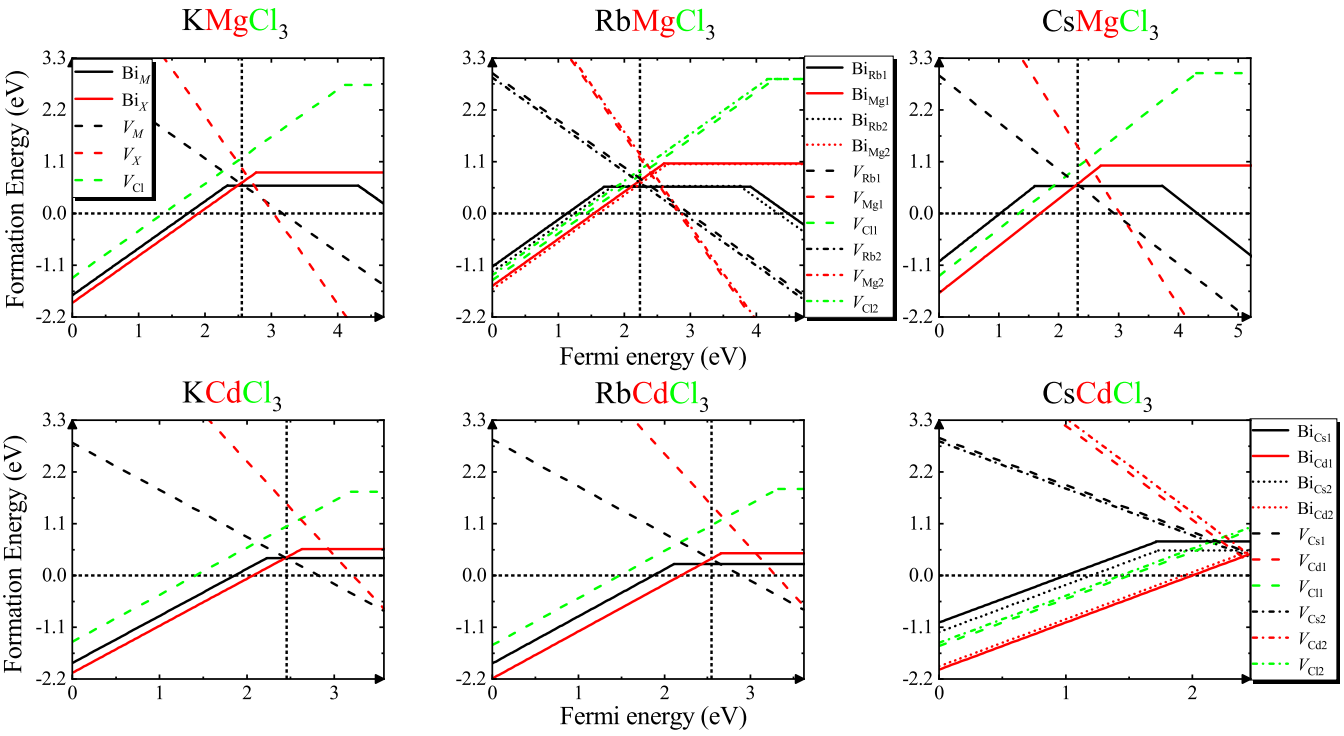

FIG. S5. Formation energies of bismuth substitutions Bi_M, Bi_X and intrinsic defects V_M, V_X, V_{Cl} in $MX\mathrm{Cl}_3$ (M = K, Rb, Cs; X = Mg, Cd) crystals as a function of Fermi level in the condition of $\Delta\mu_{\mathrm{Cl}}$ = -1.60 eV.

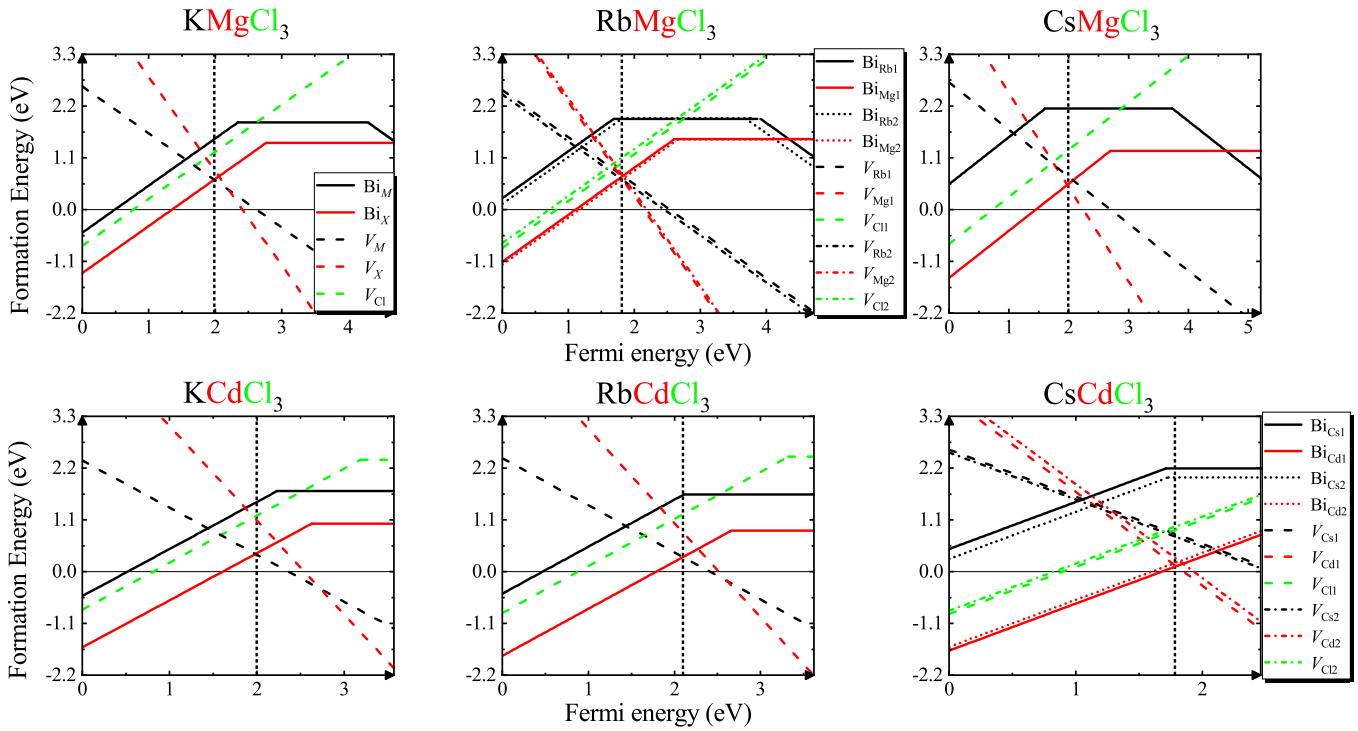

FIG. S6. Formation energies of bismuth substitutions Bi_M, Bi_X and intrinsic defects V_M, V_X, V_{Cl} in $MXCl_3$ (M = K, Rb, Cs; X = Mg, Cd) crystals as a function of Fermi level in the condition of $\Delta\mu_{MCl} = 0$ and $\Delta\mu_{Cl}$ = -1.0 eV.

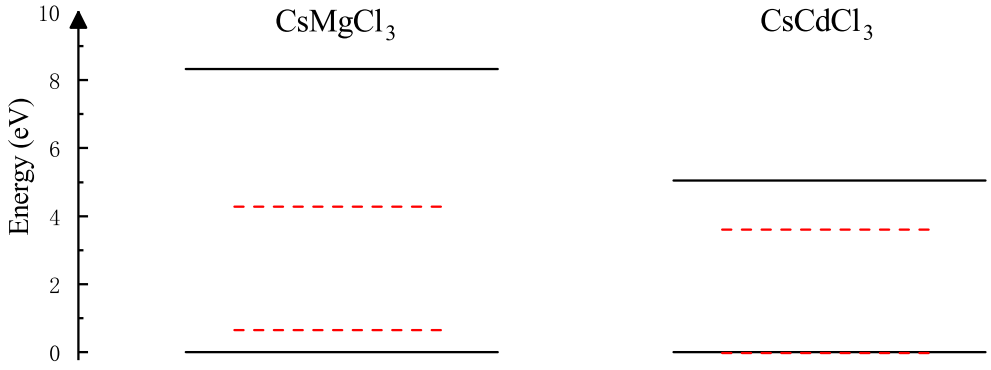

FIG. S7. The unoccupied 6s and lowest 6p KS orbital energy levels of Bi^{3+} in $CsMgCl_3$ and $CsCdCl_3$ crystals with PBE0 method.

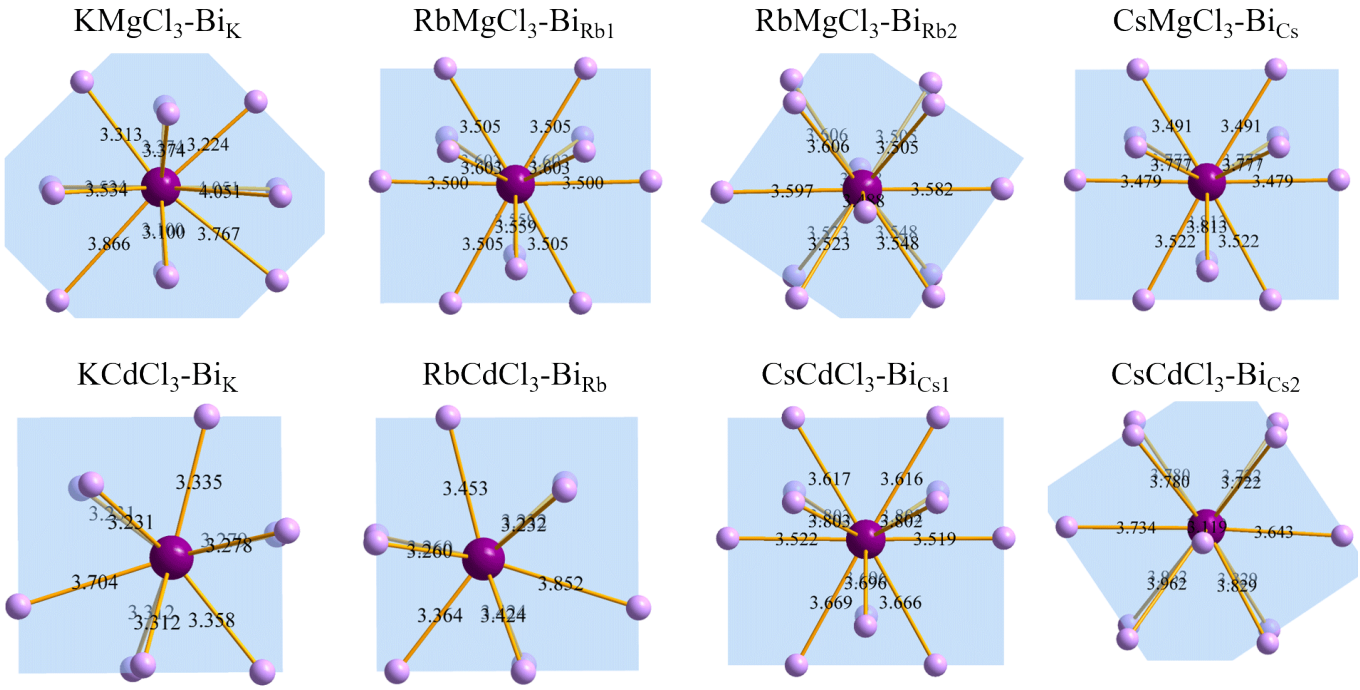

FIG. S8. Surrouding chlorine ions of bismuth substitutions Bi^0_M in different sites of a series of $MX\mathrm{Cl}_3$ crystals (in units of Å).